JOURNAL OF GEOPHYSICAL RESEARCH, VOL. 96, NO. A8, PAGES 14,183–14,187, AUGUST 1, 1991

Estimates of Solar Wind Velocity Gradients Between 0.3 and 1 AU Based on Velocity Probability Distributions from Helios 1 at Perihelion and Aphelion

SHARDA ARYA

Computer Science and Physics Department, Texas Southern University, Houston, Texas

JOHN W. FREEMAN

Department of Space Physics and Astronomy, Rice University, Houston, Texas

We have estimated the average velocity gradients for the solar wind protons by comparing the velocity probability distributions at 0.3 and at 1 AU Assuming a power law radial dependence, we find, for a full 6-year data set, that the gradients for the lowest velocity ranges are about $R^{0.1}$ to $R^{0.14}$ and that the power index decreases steadily with increasing velocity until the slope is near zero for the high-speed solar wind. However, upon examining the solar cycle dependence we find that this trend for the velocity gradient to decrease with increasing velocity is a characteristic primarily of the increasing solar activity and solar maximum period and is almost absent in the solar minimum data. The solar wind above 500 km/s during solar minimum shows an average acceleration similar to the slow wind, about 55 to 85 km/s/AU. On the other hand, winds above 350 km/s from the period of increasing solar activity and solar maximum show essentially no average acceleration beyond 0.3 AU.

1. INTRODUCTION

The two Helios spacecraft made excellent synoptic measurements of the solar wind between 0.3 and 1.0 AU [*Rosenbauer et al.*, 1977].

This paper is motivated by an examination of the hourly average proton velocity versus heliocentric distance scatterplot from Helios 1 as shown in Figure 1. This plot shows a positive overall velocity gradient. The sloped center line in Figure 1 represents the least squares fit to all of the data. This line clearly shows a positive slope. This overall positive gradient was reported by *Schwenn* [1983], who, using a slightly larger set of data, found an 11% increase in the mean velocity between 0.3 and 1 AU.

Note, however, that the top and bottom envelopes of this log-log scatterplot, which we have sketched in as straight lines, do not appear to have the same slope. These lines suggest a steeper slope for the lower velocity envelope as compared to the higher-velocity envelope. The implication is that the velocity gradient depends on velocity and that there will be a continuous change (decrease) in the gradient from lower to higher solar wind velocities.

The purpose of the present study is to obtain estimates for the velocity gradients for various velocity ranges. This is accomplished by calculating the velocity probability distributions from Helios 1 at perihelion and aphelion, dividing these distributions into velocity ranges containing equal numbers of velocity events, and comparing the shift from perihelion to aphelion in the median velocities in each corresponding range.

Previous efforts to determine large-scale velocity gradients have employed radial line-ups between the two Helios spacecraft, however, these have been restricted to a small number of opportunities and to separation distances much less than 0.7 AU. Using this method, *Schwenn et al.* [1981] reported a maximum slope of 50 km/s/AU. *Schwartz and Marsch* [1983] studied a radial line-up where the separation was 0.23 AU and found an increase in velocity of 23 km/s.

We acknowledge that the statistical method we describe here is less satisfactory than obtaining velocity gradients by radial line-ups, but we present it as an interesting alternative, because it allows us to examine velocity ranges for which line-ups are not available and also to study the full range of radial distance covered by the Helios spacecraft.

Paper number 91JA01135.
0148-0227/91/91JA-01135$02.00

2. THE VELOCITY PROBABILITY DISTRIBUTIONS

Proton velocity gradients have been determined by comparing the velocity probability distributions at perihelion and aphelion for Helios 1 from launch through 1980. Specifically, we have calculated the velocity probability distributions for the hourly averages in the two extreme distance ranges 0.3 AU to 0.4 AU and 0.96 AU to 1 AU. These distance ranges were selected to have a similar total number of data points and to represent perihelion and aphelion for Helios 1.

The hourly velocity averages from Helios 1, from the above distance ranges, were sorted into 10 km/s bins and each time the velocity fell in a particular bin the count in that bin was incremented by one. The number of counts in each bin was then divided by the total number of hourly averages to yield the probabilities. The resulting velocity probability distributions are shown in Figure 2.

From Figure 2 we see, as expected, that the bulk of the population shifts toward higher velocities and that the overall mean increases from 409 to 431 km/s between perihelion and aphelion.

Note that in the region below about 500 km/s there is a clear offset toward higher velocities for the 1 AU curve, however, this distinction disappears at higher velocities. In the high-velocity range the two probability distributions tend to coalesce and be more or less indistinguishable.

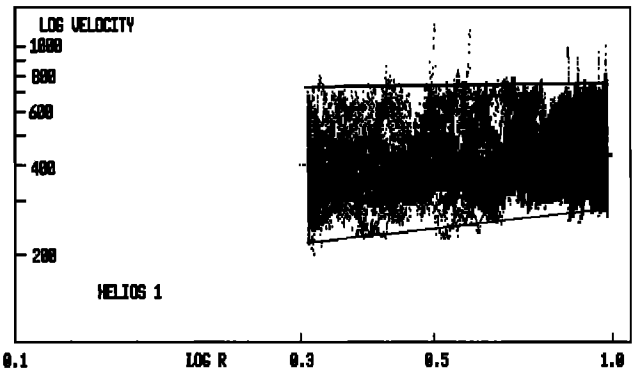

Fig. 1. Scatterplot of the Helios 1 log proton radial velocity versus log distance. The data are hourly averages from launch late in 1974 through 1980. The middle line is the result of a linear regression analysis on the entire data set and shows a 8.5% increase from 0.3 to 1 AU. The upper and lower lines have been drawn to guide the eye and illustrate that the lower envelope of points has a steeper slope than the upper envelope.

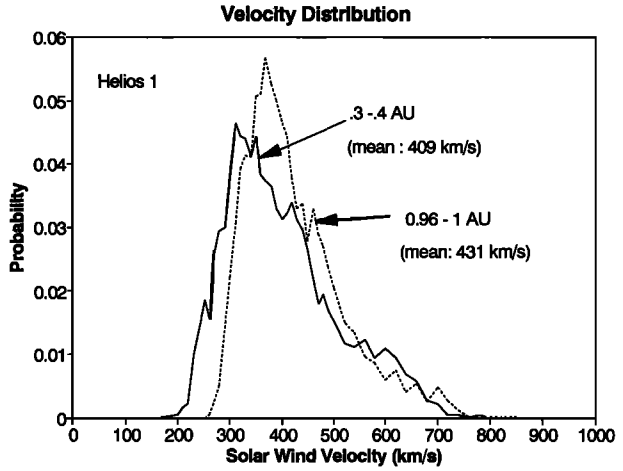

Fig. 2. Velocity probability distribution curves from perihelion and aphelion from the Helios 1 data. The probabilities have been normalized to total unity. The bin sizes are 10 km/s. The total numbers of events are 5973 and 6332 for perihelion and aphelion, respectively.

In order to examine this shift in the gradients more quantitatively the velocity number distributions at aphelion and perihelion were divided into five equal portions so that the same number of events fell in each range. There were 1195 events in each range at perihelion and 1265 events in each range at aphelion. Next, the velocity corresponding to the median of each range was determined. The shift in the median velocity for each range, from perihelion to aphelion, was then used to compute the velocity gradients, assuming a power law dependence of V on R. We computed the gradients also assuming a linear slope, however, the power law dependence is favored in view of Figure 1.

The results of this process are illustrated in Figure 3, and the numerical slopes are shown in Table 1. Table 1 also shows the median velocities and the percentage increases.

The data in Table 1 for the power law indices are also plotted in Figure 4 against the median velocities at 1 AU for each range (the run with five bins). We see that there is a steady decrease in the velocity gradients with increasing median velocity. In the highest-velocity range the index of the power law is essentially zero, whereas it is 0.1 to 0.14 in the two lowest ranges.

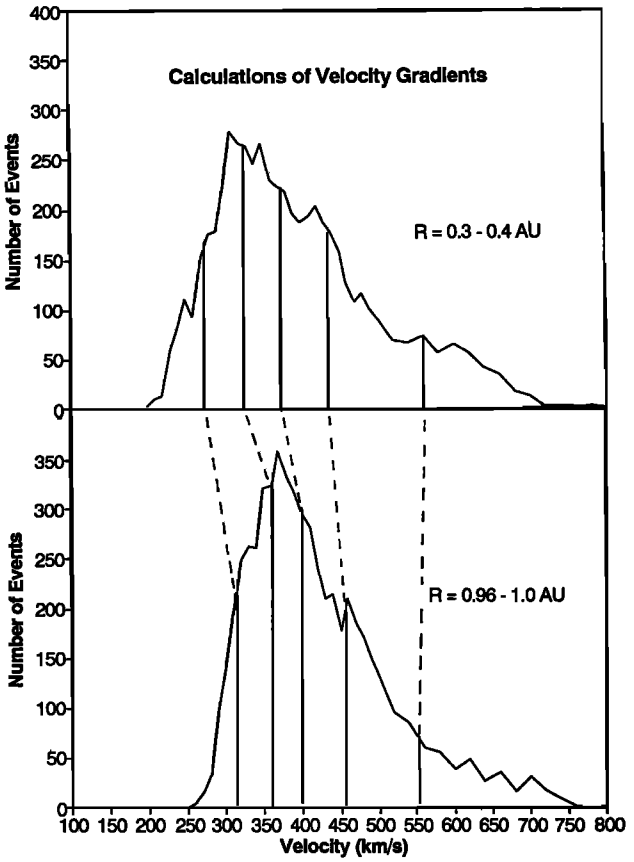

Fig. 3. Figure illustrating the offsets in the median velocities in five probability ranges, each containing equal numbers of hours of average velocities. The dashed lines connect the median velocities at perihelion and aphelion and their slants indicate the gradients in the average velocity.

2.1. Discussion of Methodology

The assumption implicit in this technique is that the velocity probability distributions map between perihelion and aphelion in a proportional manner such that the lowest 20% of the velocity events at perihelion map to the lowest 20% at aphelion, the next higher 20% at perihelion map to the next higher 20% at aphelion and so on, and that this mapping is representative of the average gradients.

In order to validate this method of estimating average gradients we have applied the same data analysis method to another solar wind parameter for which we have an independent estimate of the gradient, the solar wind proton radial temperature. The results of the temperature gradients by the present method were then compared with those obtained by a velocity sort followed by a linear regression analysis, the method used by *Schwenn* [1983] and by *Lopez and Freeman* [1986]. In order to make a direct comparison with the velocity sort temperature gradients, seven instead of five probability ranges were used. The results are shown in Table 2. Temperature gradients from the two methods from comparable median or intercept temperatures at 1 AU are shown on the same line for easy comparison. The agreement in the temperature gradients for the two methodologies is excellent. We feel that this gives validity to the method of estimating average velocity gradients used in this paper.

The errors shown in Table 1 have been estimated by using the 1 standard deviation upper and lower limits on the individual

Table 1. Velocity Gradients for Full Data Set

Range	Median Velocity at 0.3-0.4 AU	Median Velocity at 0.96-1 AU	Power Law Index,γ $(V \propto R^{\gamma})$	Linear Slope, km/s/AU	Percent Slope
1	274+-7	316+-4	0.139+-0.028	66.7+-12.8	14.2
2	326+-10	360+-5	0.096+-0.033	54.0+-17.7	9.9
3	375+-12	399+-5	0.063+-0.034	38.1+-20.6	6.2
4	436+-16	455+-7	0.041+-0.038	30.2+-27.7	4.3
5	558+-16	555+-10	-0.005+-0.033	-4.8+-29.9	-0.5

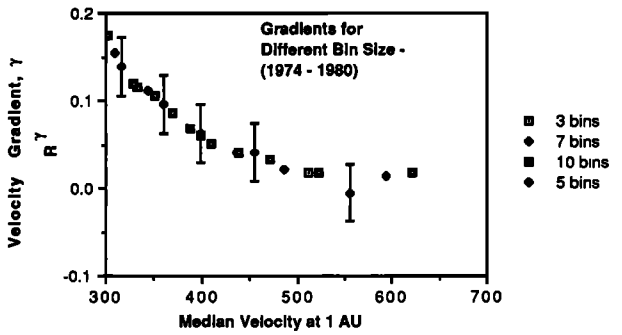

Fig. 4. The average velocity gradients as indicated by the index of the power law, plotted against the median velocity for each probability bin. This figure represents the result of four runs using a different number of probability bins. For each run, each bin contains the same number of velocity events. Error bars are shown for the run using five bins and these are the average of the errors shown in Table 1.

hourly averages and carrying out the calculation of gradients for each limit as well as the mean value. This method emphasizes the measurement error. We have also estimated the binning error by assuming that the number of events in each probability bin obeys Poisson statistics. In most cases these two error estimates were comparable although in some cases the measurement error was larger.

It could be argued that the choice of five bins might, in some way, bias the resulting gradients. In order to investigate this possibility we reran the analysis using three, seven and 10 bins of uniform probability and computed the gradients in the median velocities for each of these cases. The results of this analysis are shown in Figure 4 plotted against the median velocity at 1 AU. We see that the runs agree well and that the shape of the power-law index versus median velocity emerges as a smooth curve, sloping downward, asymptotically approaching a small positive value.

2.2. Comparison With Previous Results

Using radial line-ups, *Schwenn et al.* [1981] and *Lopez* [1985] obtained a radial gradient of about +50 km/s/AU at lower velocities. The average gradient of our four lowest ranges is 47 km/s/AU.

Schwartz and Marsch [1983] reported velocity data for the two Helios spacecraft when they were separated by 0.23 AU. From these velocities one can estimate a gradient of +100 km/s/AU, at a velocity of about 650 km/s, however, the error bars on these numbers are also consistent with zero gradient. Our study would indicate that the average gradient would be small in this velocity range.

Schwenn [1983] reported an 11% average gradient for the full Helios 1 data, from perihelion to aphelion, over a longer data interval than that used for this study. From the means in Figure 2 our average gradient is 8.5%.

TABLE 2. Comparison of Temperature Gradients

Probability Distribution		Velocity Sort		
		Lopez and Freeman [1987]		Schwenn [1983]*
Median Temperature at 1 AU, 1000 K	Temperature Gradient, γ $(T \propto R^{\gamma})$	Intercept Temperature at 1 AU, 1000 K	Temperature Gradient, γ $(T \propto R^{\gamma})$	Temperature Gradient, γ $(T \propto R^{\gamma})$
13.2 +-1.1	-1.28+-0.23	17.06 +-1.71	-1.33+-0.13	-1.33
42.2 +-1.3	-1.19+-0.09	38.82 +- 1.75	-1.22+-0.09	-1.12
90.8 +-2.1	-0.98+-0.07	81.86 +-3.93	-1.03+-0.09	-0.8
130.3 +-4.0	-0.89+-0.09	144.17+- 7.51	-0.83+-0.10	- 0.7
221.0 +-11.0	-0.69 +-0.14	200.34 +- 10.04	-0.76+-0.09	-0.6

*See Figure 6, *Schwenn* [1983].

3. Solar Cycle Variations

In order to investigate the effect of solar activity the Helios 1 data were separated into the solar minimum period, late 1974 through 1976, and the period of increasing solar activity and solar maximum, 1978 through 1980. (Synoptic plots of the solar wind velocity show that the era of long-duration corotating streams had ended by 1978 even though sunspot maximum was not reached until 1979 [*Freeman and Lopez*, 1986].) Velocity distribution curves for these two epoches are shown in Figure 5. The high velocity tail centered around 600 km/s, associated with high-speed streams, is clearly seen in the solar minimum distributions from both perihelion and aphelion but is most pronounced in the perihelion data. Both solar maximum and minimum distributions show a shift toward higher velocities at 1 AU in the lower velocity portion of the distribution but only the solar minimum distribution shows a similar shift at higher velocities.

We have applied the same type of analysis to determine velocity gradients during these two epoches, solar maximum and solar minimum, as for the full data set. The results are shown in Table 3 and in Figure 6. We see that the power law index from the solar maximum period shows a steady decline with increasing velocity, a pattern similar to the full data, however, data from the solar minimum period does not show a dramatic decrease in slope. For the solar minimum period the power index at the highest two velocities are substantially positive. The higher velocities in the solar minimum data extend to higher velocities, reflecting the presence of high-speed streams.

4. Conclusions

Evidence from the full Helios data set between the end of 1974 through 1980 indicates that the velocity gradient for the low-speed solar wind is, on the average, higher than for the high-speed wind. The low-speed wind gains, on average, about 50

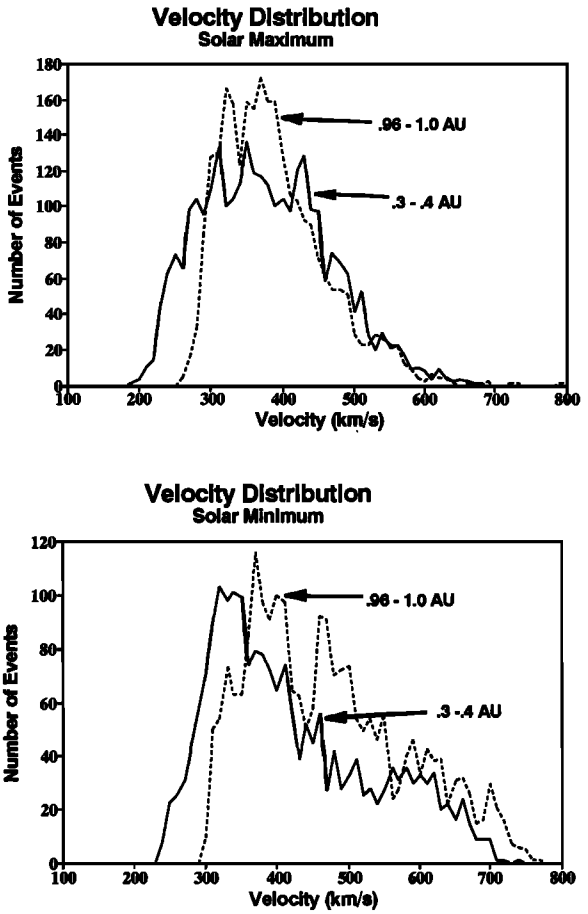

Fig. 5. The velocity distributions for perihelion and aphelion and at solar maximum and solar minimum. Both epoches show substantial offset toward higher velocities at aphelion for the low-velocity portion of the spectrum.

Table 3. Velocity Gradients for Solar Maximum and Minimum

Range	Median Velocity at 0.3-0.4 AU	Median Velocity at 0.96-1 AU	Power Law Index,γ ($V \propto R^{\gamma}$)	Linear Slope, km/s/AU	Percent Slope
			Solar Maximum (1978 - 1980)		
1	262+-10	301+-5	0.135+-0.038	62+-16	14
2	316+-9	337+-6	0.062+-0.032	33+-17	6
3	365+-13	371+-5	0.016+-0.037	10+-14	2
4	420+-17	411+-6	-0.021+-0.041	-14+-28	-2
5	489+-17	484+-9	-0.010+-0.038	-8+-30	-1
			Solar Minimum (Late 1974 - 1976)		
1	293+-6	337+-4	0.136+-0.020	70+-10	14
2	337+-8	389+-4	0.139+-0.025	83+-14	14
3	387+-11	452+-6	0.151+-0.028	103+-19	16
4	463+-16	516+-7	0.105+-0.032	84+-26	11
5	595+-18	629+-8	0.054+-0.030	54+-31	6

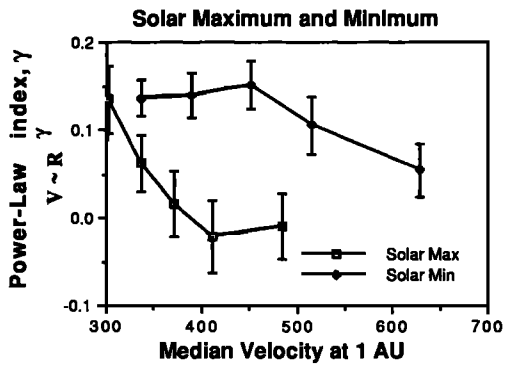

Fig. 6. Average velocity gradients as indicated by the index of the power law for the solar maximum period 1978 through 1980 and the solar minimum period late 1974 through 1976.

km/s/AU as measured between 0.3 and 1 AU and for a power law radial dependence, shows a power index of about 0.1. The velocity gradient tends to decrease with increasing velocities for the full data set.

However, results obtained by sorting the data by solar activity suggest that the decline in the gradient seen for the full data set, at higher velocities, is primarily due to contributions from the period of increasing solar activity and solar maximum and that the high-speed streams associated with solar minimum are, on average, accelerated only slightly less then the low-speed wind from the same epoch.

The decline in the velocity gradients at higher velocities, seen during increasing solar activity and solar maximum, may be characteristic of solar transient-related events. Such deceleration would be expected of explosive ejections where sustained momentum input is not possible and where slower ambient plasma ahead can slow the higher-speed wind. In contrast, solar minimum high-speed streams originating from long-duration coronal holes, with radial magnetic field configurations, would be expected to be subject to momentum input to greater radial distances.

If the average gradients given in Table 3 for the solar minimum period are characteristic of real streams, we have an estimate of the velocity addition for high-speed streams of about 55 km/s/AU between 0.3 and 1 AU.

These average velocity gradients may differ somewhat from those of actual streams, however, they may be useful for modeling and for comparison with average solar wind heating as determined by similar solar wind temperature gradients [*Marsch et al.*, 1982; *Schwenn*, 1983; *Lopez and Freeman*, 1986].

Acknowledgments. We gratefully acknowledge the contribution of the Helios data to the National Space Science Data Center by R. Schwenn, E. Marsch, H. Rosenbauer, their coworkers, and the support of the NSSDC personnel, particularly H. K. Hills and J. King. We have benefited from conversations with R. E. Lopez and T. Hill. This work was supported in part by NASA grant NGL-44-006-012 and by the Marshall Space Flight Center through Project JOVE.

The Editor thanks W. C. Feldman and another referee for their assistance in evaluating this paper.

REFERENCES

Freeman, J. W., and R. E. Lopez, Solar cycle variations in the solar wind, *Solar Wind-Magnetosphere Coupling*, edited by Y. Kamide and J. Slavin, Terra Scientific, Tokyo, 179-189, 1986.

Lopez, R. E., The two state structure of the solar wind and its influence upon protons in the inner heliosphere: Observations of Helios 1 and Helios 2, Ph.D. thesis, Rice Univ., Houston, Tex., 1985.

Lopez, R. E., and J. W. Freeman, Solar wind proton temperature-velocity relationship, *J. Geophys. Res.*, *91*, 1701-1705, 1986. (Correction to "Solar wind proton temperature-velocity relationship" and "The cold solar wind," *J. Geophys. Res.*, *92*, 13679, 1987.)

Marsch, E., K.-H. Muhlhausen, R. Schwenn, H. Rosenbauer, W. Pilipp, and F. M. Neubauer, Solar wind protons; Three-dimensional velocity distributions and derived plasma parameters measured between 0.3 and 1 AU, *J. Geophys. Res.*, *87*, 52-72, 1982.

Rosenbauer, H., R. Schwenn, E. Marsch, B. Meyer, H. Miggenrieder, M. D. Montgomery, K.-H. Muhlhausen, W. Pilipp, W. Vogues, and S. M. Zink, A survey of initial results of the Helios plasma experiment, *J. Geophys. Res.*, *42*, 561-580, 1977.

Schwartz, S. J., and E. Marsch, The radial evolution of a single solar wind parcel, *J. Geophys. Res.*, *88*, 9919-9932, 1983.

Schwenn, R., The average solar wind in the inner heliosphere: Structure and slow variations, solar wind, five, *NASA Conf. Publ., CP-2280*, 489-505, 1983.

Schwenn, R., H. Rosenbauer, and E. Marsch, Two states of the solar wind at the time of solar activity minimum, II, Radial gradients of plasma parameters in fast and slow streams in *Solar Wind Four*, Rep. MPAE-W-100-81-31, pp. 126-130, Max-Planck-Institute für Aeronomic, Kattenburg-Lindau, Federal Republic of Germany, 1981.

S. Arya, Computer Science and Physics Department, Texas Southern University, Houston, TX 77004.

J. W. Freeman, Department of Space Physics and Astronomy, Rice University, Houston, TX 77251.

(Received November 8, 1990;
revised February 18, 1991;
accepted April 10, 1991.)